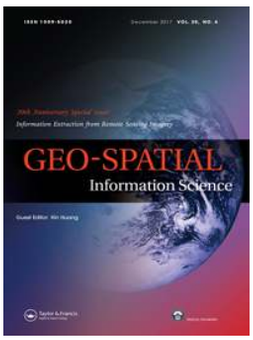

Geo-spatial Information Science

ISSN: 1009-5020 (Print) 1993-5153 (Online) Journal homepage: https://www.tandfonline.com/loi/tgsi20

A novel mathematical morphology based algorithm for shoreline extraction from satellite images

C. A. Rishikeshan & H. Ramesh

To cite this article: C. A. Rishikeshan & H. Ramesh (2017) A novel mathematical morphology based algorithm for shoreline extraction from satellite images, Geo-spatial Information Science, 20:4, 345-352, DOI: 10.1080/10095020.2017.1403089

To link to this article: https://doi.org/10.1080/10095020.2017.1403089

GEO-SPATIAL INFORMATION SCIENCE, 2017
VOL. 20, NO. 4, 345–352
https://doi.org/10.1080/10095020.2017.1403089

Taylor & Francis
Taylor & Francis Group

A novel mathematical morphology based algorithm for shoreline extraction from satellite images

C. A. Rishikeshan and H. Ramesh

National Institute of Technology, Karnataka, Surathkal, India

ABSTRACT

Shoreline extraction is fundamental and inevitable for several studies. Ascertaining the precise spatial location of the shoreline is crucial. Recently, the need for using remote sensing data to accomplish the complex task of automatic extraction of features, such as shoreline, has considerably increased. Automated feature extraction can drastically minimize the time and cost of data acquisition and database updating. Effective and fast approaches are essential to monitor coastline retreat and update shoreline maps. Here, we present a flexible mathematical morphology-driven approach for shoreline extraction algorithm from satellite imageries. The salient features of this work are the preservation of actual size and shape of the shorelines, run-time structuring element definition, semi-automation, faster processing, and single band adaptability. The proposed approach is tested with various sensor-driven images with low to high resolutions. Accuracy of the developed methodology has been assessed with manually prepared ground truths of the study area and compared with an existing shoreline classification approach. The proposed approach is found successful in shoreline extraction from the wide variety of satellite images based on the results drawn from visual and quantitative assessments.

ARTICLE HISTORY
Received 24 May 2017
Accepted 24 September 2017

KEYWORDS
Feature extraction; shoreline detection; satellite image processing; remote sensing; mathematical morphology

1. Introduction

Delineation and extraction of coastlines from remote sensing imagery is a vital task and useful for various application fields, such as coastal zone management, coastline erosion monitoring, GIS database updating, watershed definition, flood and other disaster management and the evaluation of water resources. Recently, the need for using remote sensing data to perform the task of automated extraction of features has increased significantly. Automated feature extraction can drastically minimize the time and cost of data acquisition and database updating. Remote sensing techniques, different from the exhaustive and expensive field evaluations (Addo, Jayson-Quashigah, and Kufogbe 2011), have prominent advantages of being macroscopic, comprehensive, high-frequency, dynamic, and low-cost. The automated collection of this information is difficult, complex and time consuming, when people use conventional ground survey methods. Moreover, it is highly dependent on the morphological characteristics of the coastline (like rock cliffs, sandy beaches). Therefore, rapid and replicable techniques are required to monitor coastline retreat or aggradation, and update coastline maps (Puissant, Lefèvre, and Weber 2008).

Satellite image feature extraction has been studied by several researchers. Gens (2010) extensively reviewed the current status of the use of remote sensing for the detection, extraction and monitoring of coastlines by first checking the shoreline indicators and then the remote sensing techniques used for coastline monitoring. Liu and Jezek (2004a) performed delineation of the complete coastline of Antarctica using SAR imagery. Braga et al. (2013) obtained the digital number (DN) value of the threshold with a simple geometric Equation proposed by La Monica et al. (2008). All the pixels lesser than the designated threshold were classified as water; all the pixels higher than the designated threshold were classified as land. Finally the rough shoreline is extracted with the edge detection technique, based on the identified threshold. Bo, Delleplane, and de Laurentiis (2001) proposed a texture analysis-based technique for shoreline extraction from remotely sensed imageries. Di et al. (2003) used the image segmentation algorithm proposed by Comaniciu and Meer (2002) to detect shoreline. Giannini and Parente (2014) described that automated high-resolution satellite images extraction of the coastline is more complex, because of the reduced pixel dimensions that require greater attention to distinguish different classes such as sea and soil. They also proposed an object-based approach for instantaneous coastline extraction from QuickBird data-set. Bagli and Soille (2003) suggested a morphological

CONTACT C. A. Rishikeshan rishikesh.ca@gmail.com

segmentation-assisted automated method for coastline extraction. A sea–land separation method and its corresponding shoreline detection method were proposed for interpreting multispectral remote sensing images by considering both spectral attributes and texture attributes (Wang, Zhang, and Ma 2010). Huang et al. (2016) proposed scale-span differential profiles (i.e. generalized differential morphological profiles, GDMPs) to obtain the complete differential profiles. GDMPs can describe the complete shape spectrum and quantify the difference between arbitrary scales, which is more appropriate for representing the multiscale characteristics and complex landscapes of remote sensing image scenes.

To locate the position of shoreline optimally and reliably, many types of methods have been proposed by numerous researchers. These includes the application of supervised classification (Hoeke, Zarrillo, and Synder 2001; Nguyen et al. 2013; Hoonhout et al. 2015), unsupervised classified images (Guariglia et al. 2006; Ekercin 2007; Huang et al. 2014), and several thresholding-assisted methods (White, Asmar, and Hesham 1999; Qu and Wang 2002; Liu and Jezek 2004b; Bayram et al. 2008; Maiti and Bhattacharya 2009; Kuleli et al. 2011). Approaches focusing on hard classification render each pixel either as sea or land. These approaches are less effective in delineating the shoreline and in several instances, which may lead to large proportion of misclassification. Huang et al. (2014) conducted a detailed comparison between unsupervised and supervised methods and showed that some unsupervised feature extraction methods have the potential to provide better results than the supervised ones.

In the traditional classification, only DN of pixels are considered. But with the mathematical morphology (MM) strategies, one could additionally consider shape, neighborhood, size, and other features of the object. The shape-oriented processing capability of the MM approach has rendered it popular with remote sensing images. Moreover, existing MM-based approaches do not give the flexibility to work with any resolution imageries and an option to feed result governing variables dynamically. In this research, we propose an MM-based approach for the extraction of shorelines from higher and moderate resolution imageries. In an MM approach, the value of each pixel in the resultant image is based on an assessment of the matching pixel with its neighbors in the input image. By picking the shape and size of the neighborhood, one can make a morphology-assisted operation (useful to particular shapes, such as shorelines) in a given image. A set of powerful MM-driven operations (such as opening, closing, top-hat, bot-hat) and reconstruction-driven operations were applied at multiple times and on multiple instances to delineate shorelines. Preservation of actual size and shape of the shorelines, semi-automation, minimal turnaround time, and single band adaptability are the salient features of this work. The proposed approach is effective and useful for the extraction of shorelines from several varieties of satellite imageries. The accuracy of our methodology has been assessed with manually prepared ground truths of a study area and compared with traditional shoreline classification approaches.

2. Technical background

MM was introduced in the works of Matheron (1975) and was used by researcher Serra (1982) for image analysis. It contributes a wide range of operators to image processing domain, all grounded around a few mathematical concepts from set theory. The fundamental morphological operations have been extensively discussed in image processing literatures, like those of Gonzalez and Woods (2002), Seul, O'Gorman, and Sammon (2000), Soille (2004), and Parker (1996). Dilation and erosion are the two primary morphological operations. Dilation is a Minkowski addition and can be expressed as a union of translated point sets. Erosion is a Minkowski subtraction which is the intersection of translated point sets.

Grayscale morphology can be expressed in detail as: If $f(p,q)$ denotes the input grayscale image, $\mathrm{se}(p,q)$ denotes a structuring element (SE), and Df and Dse denote the field of function $f(p,q)$ and $\mathrm{se}(p,q)$, respectively.

For the grayscale MM, dilation operation for grayscale image $f \oplus \mathrm{se}(p,q)$ is:

$$\mathrm{Max}\,[f(p-p', q-q') + \mathrm{se}(p', q')] \tag{1}$$

where $\{(p-p',\ q-q' \in \mathrm{D}f),\ (p',\ q' \in \mathrm{Dse})\}$; the erosion operation for grayscale image $f \ominus \mathrm{se}(p,q)$ is:

$$\mathrm{Min}\,[f(p+p', q+q) - \mathrm{se}(p', q')] \tag{2}$$

where $\{(p+p',\ q+q' \in \mathrm{D}f),\ (p',\ q' \in \mathrm{Dse})\}$.

Grayscale MM opening involves erosion operation followed immediately by dilation operation using the same SEs. Grayscale MM closing involves dilation operation followed immediately by erosion operation using the same SEs (Deng et al. 2014). In an MM approach, the value of each pixel in the resultant imagery is determined by an assessment of the matching pixel in the input imagery with its neighbors. By picking the shape and size of the neighborhood, a morphology-assisted operation (useful to particular shapes in a given image) can be made (de Castro and Centeno 2010). The coastal line extraction using remote sensing and GIS tools got substantial attention over the past few decades. It is very important to extract those features of large area by efficient methods and strategies for the mapping, assessment, etc.

3. Data and methods

3.1. Data

This investigation uses a wide set of satellite imageries to identify the performance of the proposed approach: data-sets including very high-resolution panchromatic

Table 1. Specification of data-set.

Sl. No.	Satellite and sensor	Spatial resolution /m	Source agency	Area of interest	Date of procurement (Date of pass)
1.	Cartosat-2, PAN	0.8	NRSC	Mangalore, India	12 NOV 2008
2.	Cartosat-1, PAN (Tile-532-338)	2.5	NRSC	Mangalore southern coast, India	16 FEB 2012
3.	Cartosat-1, PAN (Tile-530-334)	2.5	NRSC	Mangalore northern coast, India	14 NOV 2014
4.	Resource sat-2, LISS IV	5.8	NRSC	Mangalore, India	06 FEB 2016
5.	Landsat 8, ETM+	30.0	USGS	Mangalore northern coast, India	11 JAN 2015

(PAN) data of 0.8 meter, moderate resolution Resource sat-2 LISS IV 5.8 meter data, and low-resolution Landsat ETM + 30 meter data. The algorithm code is written in MATLAB environment and requires SDC MM toolbox for execution. The important data-sets used for this investigation is procured from various sources and agencies mentioned in Table 1.

3.2. Algorithm

Input: An N×N matrix sized satellite input image (f1).
Output: An N×N matrix sized extracted output image (X).

1. Start
2. Procurement and registration of the satellite image.
3. Pre-processing operations to suppress nonlinear objects and noises such as salt and pepper.
4. SEs (SE1 to SE3), pixel size (P, to remove noises /non shore objects) and threshold (th1 to th5) declarations and initializations for processing activities.
5. Prompt for spatial resolution of input satellite images: input 1 for very high (<1 m), 2 for high (1–5 m), 3 if moderate (5–25 m), 4 if sparse (>25 m).
6. Computation of matching top-hat and bot-hat algebra; (f2 = f1+tophat(f1, SE1)) – bothat(f1, SE1).
7. Opening by reconstruction; f3=R_{fo}(f2, SE2).
8. Thresholding
   If (auto threshold) then
      switch Res
      case '1': X1 = im2bw(f3, th1);
      case '2': X1 = im2bw(f3, th2);
      case '3': X1 = im2bw(f3, th3);
      case '4': X1 = im2bw(f3, th4);
      otherwise
      X1 = im2bw(f3, th5);
   End
   Else (manual threshold)
      prompt = 'Please enter threshold value'
      X1 = input(prompt);
      X1 = im2bw(f3, X1);
9. Closing by reconstruction; X = R_{fc}(X1, SE3, mmsebox).
10. Binary area open; bwareaopen(X, P), noise removal (non-shores)
11. Display extracted outcome and save resultant imagery.
12. End.

The methodological flowchart of this work is presented in Figure 1. The acquired image initially undergoes various pre-processing operations to rectify radiometric and geometric errors. Apart from this, we have chosen completely cloud-free data-sets. As pre-processing operations, a median filtering (such as $f1$ = MF(fg, [3, 3])) is applied to suppress non-linear objects and noises such as salt and pepper. The declaration and initialization of SE and threshold which governs important processing activities are performed before the execution of the algorithm. Moreover, the SEs and threshold values initialized have a greater significance; their slight variation changes the entire shoreline extraction result and accuracy. This binary operation (opening) attempts to

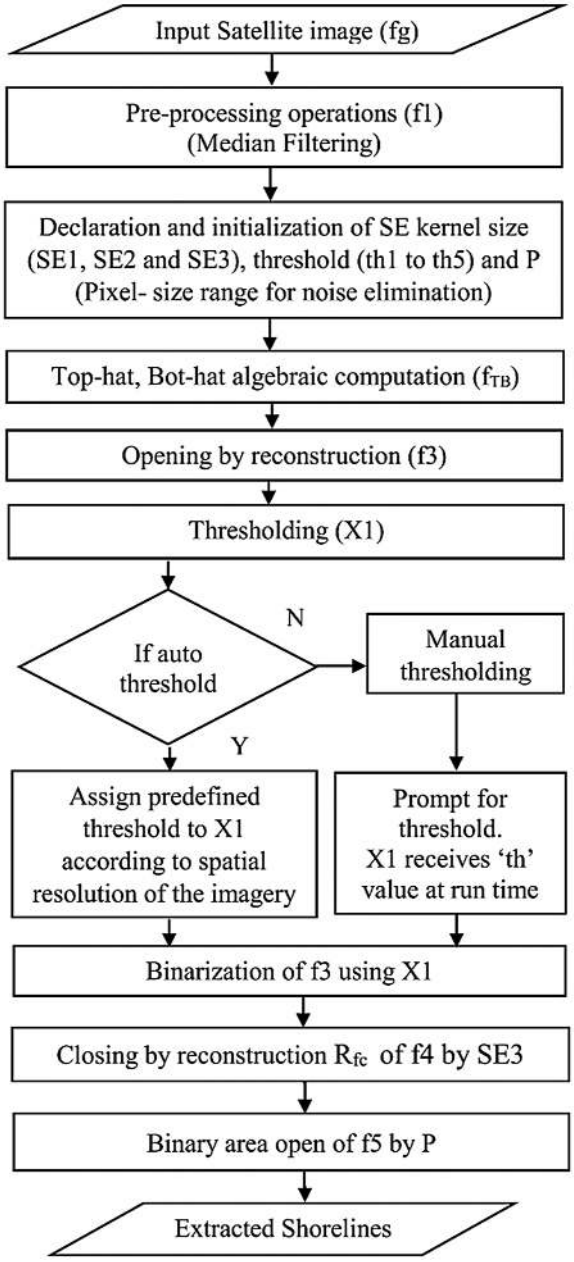

Figure 1. Flowchart of the proposed approach for shoreline extraction.

open small gaps between touching objects in an image. Also, it can be explained as a process that destroys edges. This concept is directly applied to the analyzed coastal image to get rid of the edges present in land, while preserving the coastline. The closing operation closes or fills the gaps between objects. Opening will act over neighboring pixels, destroying the edges in the touching

objects of the image. Then the image is smoothed, while the strongest edges remain. A series of MM operations were applied, starting with powerful MM computation of matching top-hat and bot-hat algebra and opening by reconstruction, followed by thresholding operations either automatically or manually. Then the algorithm aims to isolate unwanted objects that are irrelevant in shoreline delineation through closing by reconstruction and binary area open operation (with a pixel size P) with the threshold image.

MM reconstruction is advantageous and is a good exercise for extracting substantial details about shapes in an image (Gonzalez and Woods 2002). Since we use MM reconstruction driven operations, the actual size and shape of the objects in the outcome remain unchanged. The distinctive properties of such processing are based on two images; a marker image, a mask rather than a single image and an SE. The execution repeats until the image no longer alters. MM reconstruction can be used to detect and delineate marked objects, find bright areas bounded by dark pixels, detect or eliminate objects touching the image boundary, find or fill in object gaps, filter out spurious high or low points, and execute many other operations.

The ground truths are prepared by combining the knowledge of the user via field visit and manual digitization. Apart from this, Google earth verification and correction at pixel and object level in an iterative fashion to obtain maximum possible accuracy is performed. A supervised classification was performed using shore and non-shore signatures. The signatures were grouped as either non-shore or shore region. Sufficient numbers of signatures for shore regions and non-shore regions were collected to ensure better classification accuracy.

3.3. Evaluation metrics for performance

Comparison of extracted shorelines and manually delineated shorelines are performed pixel by pixel. Sample pixels in the image are categorized into four types: true positive (TP): the pixel belongs to shore in both the manual and extracted result, true negative (TN): the pixel belongs to background in both the manual and extracted result, false positive (FP): the pixel is incorrectly labeled as shore in the extracted result, and false negative (FN): the pixel is incorrectly labeled as background in the extracted result (Zhou et al. 2014).

To evaluate the performance of the system, accuracy has been computed based on the number of correctly detected characters in an image. F-Score in Equation (3), accuracy in Equation (4), and Matthew's correlation coefficient (MCC) in Equation (5) are the metrics used to evaluate the system performance.

$$\text{F-score} = 2TP/(FP + TP + P) \tag{3}$$

$$\text{Accuracy} = \frac{TP + TN}{P + N} \tag{4}$$

$$\text{MCC} = \frac{TP \times TN - FP \times FN}{\sqrt{((TP + FP) \times (TP + FN) \times (TN + FP) \times (TN + FN))}} \tag{5}$$

4. Results and discussion

The proposed approach is tested with imageries of different region of interest (ROI) with varying areal coverage and images acquired from several sensors with different acquisition dates and with higher spatial resolution. This section describes the results drawn from different sets of the input imageries including visual, qualitative and quantitative assessments. The results of this analysis are also compared with the results of the existing traditional classification outcome.

Figures 2–6 illustrate the different input data-sets, ground truth image, MM algorithm processing stage, results drawn from existing classification approach and output drawn from proposed MM approach.

Figure 2(d) and (e) illustrate the performance of an existing classification approach and the proposed MM algorithm with Cartosat-1 (Tile-532-338) imagery. The

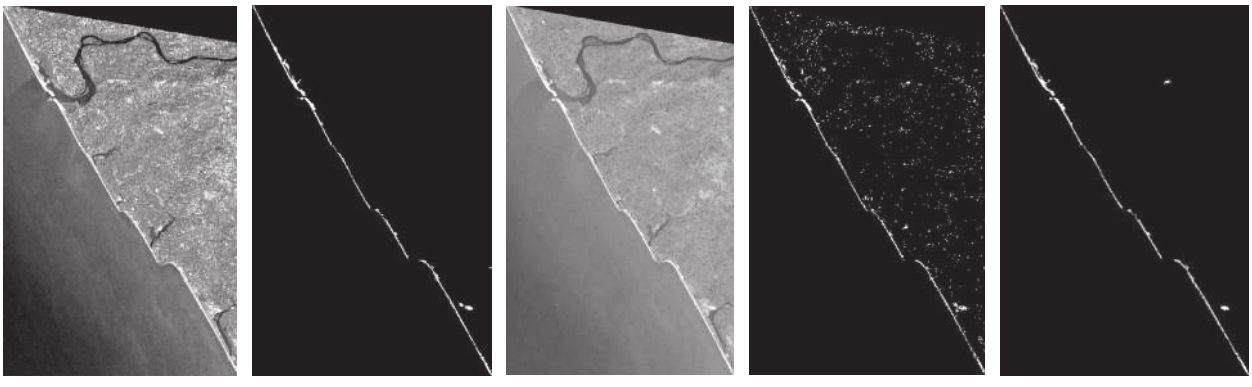

Figure 2. Illustration of results with Cartosat-1, PAN (Tile-532-338) imagery. (a) Original image, (b) Ground truth, (c) MM processed image (intermediate stage), (d) Classification outcome, (e) Proposed MM algorithm outcome.

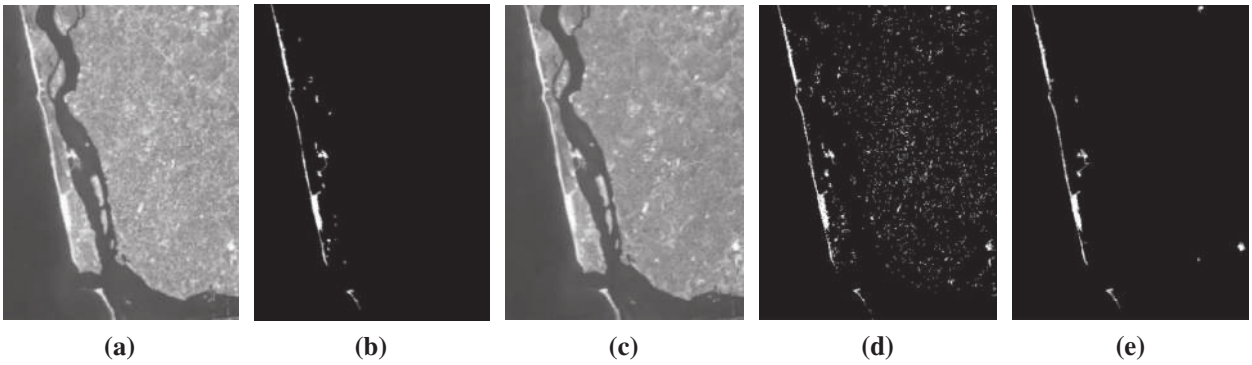

Figure 3. Illustration of results with Cartosat-2 imagery (a) Original image, (b) Ground truth, (c) MM processed image (intermediate stage), (d) Classification outcome, (e) Proposed MM algorithm outcome.

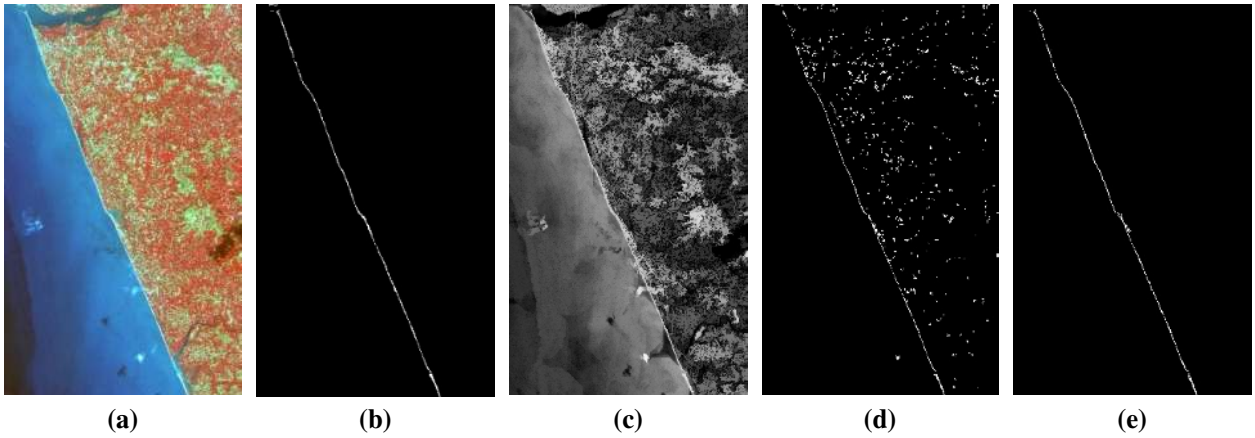

Figure 4. Illustration of results with Resource sat-2, LISS IV imagery. (a) Original image, (b) Ground truth, (c) MM processed image (intermediate stage), (d) Classification outcome, (e) Proposed MM algorithm outcome.

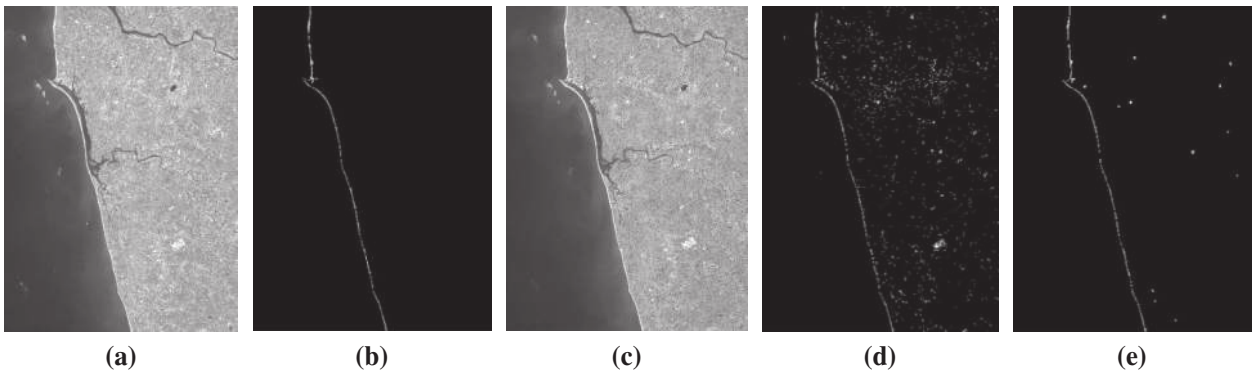

Figure 5. Illustration of results with Cartosat 1, PAN (Tile-530-334) imagery. (a) Original image, (b) Ground truth, (c) MM processed image (intermediate stage), (d) Classification outcome, (e) Proposed MM algorithm outcome.

proposed algorithm extracts shorelines with a better accuracy of 99.91% compared to the accuracy of 98.97% of shoreline classification approach. The MCC (0.94695) and F-score (0.94737) values are also marginally better than those of the traditional classification approach.

Figure 3(e) illustrates the algorithm performance with Cartosat-2 imagery covering Mangalore shores and Netravathi River segments. Here, the proposed algorithm is able to extract shorelines with 99.79% accuracy and satisfactory MCC (0.89568) and F-score (0.89663) values. Even though traditional shoreline classification approach has an accuracy of 98.15%, its MCC and F-score values are lower than 0.6 due to misclassifications.

Figure 4(e) illustrates the performance of the algorithm with LISS IV imagery of coastal regions of Northern Mangalore. Here, accuracy of 99.88% is achieved by the proposed algorithm compared to 98.85% by existing classification approach. MCC and F-score values (0.8689 and 0.8680) are observed for the proposed

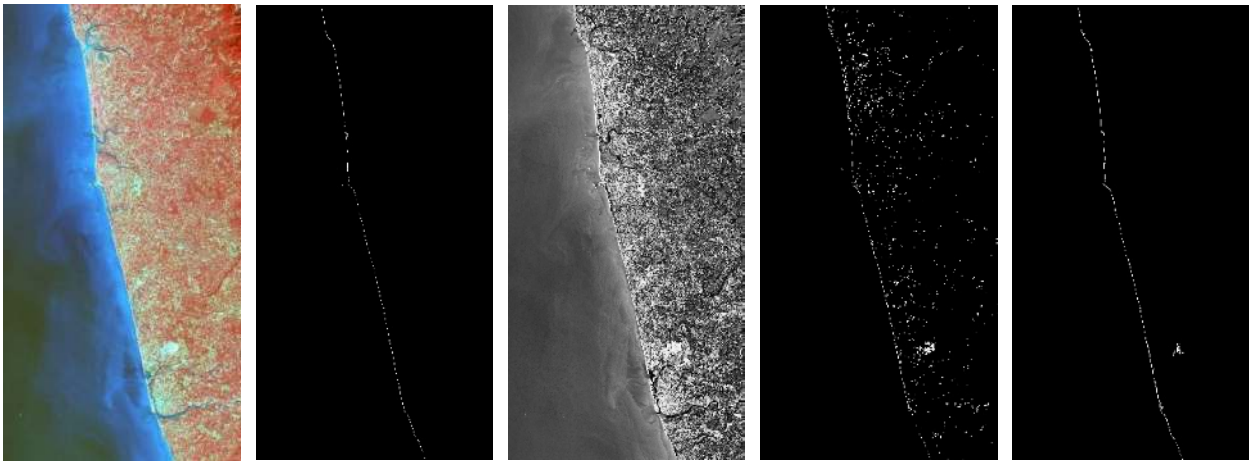

Figure 6. Illustration of results with Landsat ETM + sensor imagery. (a) Original image, (b) Ground truth, (c) MM processed image (intermediate stage), (d) Classification outcome, (e) Proposed MM algorithm outcome.

Table 2. Accuracy assessment of the proposed MM approach.

Sensor and ROI description	TP (feature)	FP	TN (background)	FN	F-score	MCC	Accuracy
Cartosat-2, PAN	470,275	47,498	52,904,280	60,929	0.896 63	0.895 68	0.997 97
Cartosat-1, PAN (Tile-532-338)	285,895	17,426	36,154,604	14,335	0.947 37	0.946 95	0.999 12
Cartosat-1, PAN (Tile-530-334)	240,917	71,419	86,907,650	10,794	0.854 24	0.858 78	0.999 05
Resource sat-2, LISS IV	74,394	6292	19,993,870	16,324	0.868 05	0.868 99	0.998 87
Landsat 8, ETM+	36,497	48,011	27,884,335	3613	0.585 74	0.626 19	0.998 15

Table 3. Accuracy assessment of existing shoreline classification approach.

Sensor and ROI description	TP (feature)	FP	TN (background)	FN	F-score	MCC	Accuracy
Cartosat-2, PAN	509,278	966,121	51,985,657	21,926	0.507 60	0.569 41	0.981 520
Cartosat-1, PAN (Tile-532-338)	256,139	328,471	35,843,559	44,091	0.578 94	0.607 27	0.989 780
Cartosat-1, PAN (Tile-530-334)	216,435	893,029	86,086,040	35,276	0.859 85	0.406 68	0.989 358
Resource sat-2, LISS IV	68,414	207,940	19,792,222	22,304	0.372 75	0.428 11	0.988 539
Landsat 8, ETM+	37,263	246,138	27,686,208	2847	0.230 36	0.215 75	0.974 895

algorithm. As to the existing classification approach, it is observed to be 0.3727 and 0.4281.

Figure 5 illustrates the performance of the algorithm with Cartosat-1 imagery of northern coastal regions of Mangalore. In this case, the algorithm is able to detect shorelines with 99.90% percentile accuracy; and for MCC and for F-score, the values 0.85878 and 0.85424 are recorded.

Figure 6 illustrates the performance of the algorithm with Landsat 8, ETM + imagery. The proposed algorithm extracts shoreline with an accuracy of 99.81% compared to the accuracy of 97.48% of traditional shoreline classification approach. Since the areal extent is wide, visually the shoreline appears very thin. Numerous other objects with reflections resembling shoreline pixels were present in the imagery. These reflections led to a reduction of other performance measures such as F-score and MCC. The traditional shoreline classification approach shows lesser amount of MCC and F-score values of 0.21575 and 0.23036, respectively.

The performance of the proposed extraction approach and existing shoreline classification approach are depicted in Tables 2 and 3, respectively. Compared to the proposed MM approach, there is increased number of FP and decreased TP pixels in the existing classification method. Similarly, TP pixels recorded a marginal lower count compared to proposed MM approach. Among all the data-sets employed except Cartosat-2 PAN imagery, the proposed algorithm excels in TP pixels. The Cartosat-1 (Tile-532-338) imagery shows highest overall performance (above 0.9) in terms of accuracy, MCC, and F-score. Among other data-sets, Cartosat-2 imagery also shows similar value of accuracy with better MCC and F-scores values. The lowest performance (MC: 0.62619 and F-score: 0.58574) observed is with Landsat 8 imagery. The reduction in F-score and MCC values may be due to the presence of objects with reflections resembling shoreline pixels in the imagery. Similarly, wider areal coverage is also accounted for the reduction in performance of Landsat 8 imagery. Here, slight variations of spatial resolution of imagery do not deteriorate the performance, whereas, large variations affects the performance on a larger scale, since the shoreline appears very thin in moderate and coarse resolution imageries. As compared to the manual digitization, our algorithm takes less time for processing. The turnaround

time is only few minutes, whereas it finishes within a few minutes for very small coastal areas.

5. Conclusions

In shoreline extraction, automated and replicable techniques play a vital role in updating coastline maps, to evaluate the spatial and temporal evolution of alterations due to natural and anthropogenic events, especially for large areas. In this research, the applications and effectiveness of MM-assisted approach for the extraction of shorelines from several varieties of satellite images have been presented. The accuracy of the developed methodology has been assessed with manually prepared ground truths, which reveals that our algorithm performs better with different imagery data-sets in comparison with the existing methods.

Notes on contributors

C. A. Rishikeshan received the Computer Engineering degree in 2009 from Institution of Engineers (IEI), India and MTech. degree in remote sensing and GIS from Maulana Azad National Institute of Technology (MANIT) Bhopal, India, in 2011. From Aug. 2011 to Sep. 2012, he was an application developer in IBM India Pvt. Ltd. at Bangalore. Later he moved to Amrita University and served as an assistant professor till 2014. He is currently working toward the PhD degree at the National Institute of Technology Karnataka, India. His research interests include remote sensing, satellite image processing, and algorithms for feature/object extraction and DEM analysis.

H. Ramesh received Bachelor of Engineering (BE) degree in Civil Engineering from Sir M Visvesvaraya Institute of Technology, Bengaluru, India, in 1999, master of technology (MTech.) degree in Hydraulics from the National Institute of Engineering, Mysore, India in 2002, and PhD degree in Water Resources Engineering from National Institute of Technology in 2008. At the start of 2007, he first joined as a research associate at CISED/ATREE, Bengaluru. Since 2009, he has been working as an assistant professor at National Institute of Technology Karnataka. His main research interests include water resources, hydrology, climate change, application of remote sensing and GIS, hydro and ocean wave energy.

ORCID

C. A. Rishikeshan http://orcid.org/0000-0002-4986-6636

References

Addo, K. A., P. N. Jayson-Quashigah, and K. S. Kufogbe. 2011. "Quantitative Analysis of Shoreline Change Using Medium Resolution Satellite Imagery in Keta, Ghana." *Marine Science* 1 (1): 1–9. doi:10.5923/j.ms.20110101.01.

Bagli, S. and P. Soille. 2003. "Morphological Automatic Extraction of Coastline from PAN-European Landsat TM Images." The Fifth International Symposium on GIS and Computer Cartography for Coastal Zone Management, Genoa, Italy, October 16–18.

Bayram, B., U. Acar, D. Seker, and A. Ari. 2008. "A Novel Algorithm for Coastline Fitting through a Case Study over the Bosphorus." *Journal of Coastal Research* 24 (4): 938–991. doi:10.2112/07-0825.1.

Bo, G., S. Delleplane, and R. de Laurentiis. 2001. "Coastline Extraction in Remotely Sensed Images by Means of Texture Features Analysis." Geoscience and Remote Sensing Symposium, IGARSS'01, the IEEE International, Sydney, NSW, Australia, July 9–13.

Braga, F., L. Tosi, C. Prati, and L. Alberotanza. 2013. "Shoreline Detection: Capability of COSMO-SkyMed and High-resolution Multispectral Images." *European Journal of Remote Sensing* 46 (1): 837–853. doi:10.5721/EuJRS20134650.

Deng, C., Y. Chen, H. Bi, and Y. Han. 2014. "The Improved Algorithm of Edge Detection Based on Mathematics Morphology." *International Journal of Signal Processing, Image Processing & Pattern Recognition* 7 (5): 309–322.

de Castro, F. S. P. and J. A. S. Centeno. 2010. "Road Extraction from ALOS Images Using Mathematical Morphology." ISPRS TC VII Symposium, Vienna, Austria, July 5–7.

Comaniciu, D., and P. Meer. 2002. "Mean Shift: A Robust Approach toward Feature Space Analysis." *IEEE Transactions on Pattern Analysis & Machine Intelligence* 24 (5): 603–619.

Di, K., J. Wang, R. Ma, and R. Li. 2003. "Automatic Shoreline Extraction from High-resolution IKONOS Satellite Imagery." ASPRS Annual Conference, Anchorage, Alaska, May 5–9.

Ekercin, S. 2007. "Coastline Change Assessment at the Aegean Sea Coasts in Turkey Using Multi-temporal Landsat Imagery." *Journal of Coastal Research* 233 (3): 691–698. doi:10.2112/04-0398.1.

Gens, R. 2010. "Remote Sensing of Coastlines: Detection, Extraction and Monitoring." *International Journal of Remote Sensing* 31 (7): 1819–1836. doi:10.1080/01431160902926673.

Giannini, M. B., and C. Parente. 2014. "An Object Based Approach for Coastline Extraction from Quickbird Multispectral Images." *International Journal of Engineering & Technology (IJET)* 6 (6): 2698–2704.

Gonzalez, R. C., and R. E. Woods. 2002. *Digital Image Processing*. 2nd ed. New Jersey: Addison-Wesley.

Guariglia, A., A. Buonamassa, A. Losurdo, and R. Saladino. 2006. "A Multisource Approach for Coastline Mapping & Identification of the Shoreline Changes." *Annals of Geophysics* 49 (1): 295–304. doi:10.4401/ag-3155.

Hoeke, R. K., G. A. Zarrillo, and M. Synder. 2001. "A GIS Based Tool for Extracting Shorelines Positions from Aerial Imagery (BEACHTOOLS)." Technical Note ERDC/CHL CHETN-IV-37. https://www.researchgate.net/publication/266348090_A_GIS_Based_Tool_for_Extracting_Shoreline_Positions_from_Aerial_Imagery_BeachTools.7

Hoonhout, B. M., M. Radermacher, F. Baart, and L. J. P. van der Maaten. 2015. "An Automated Method for Semantic Classification of Regions in Coastal Images." *Coastal Engineering* 105: 1–12. doi:10.1016/j.coastaleng.2015.07.010.

Huang, X., X. Guan, J. A. Benediktsson, L. Zhang, and J. Li. 2014. "Multiple Morphological Profiles from Multicomponent-base Images for Hyperspectral Image Classification." *IEEE Journal of Selected Topics in Applied Earth Observations & Remote Sensing* 7 (12): 4653–4669.

Huang, X., X. Han, L. Zhang, J. Gong, W. Liao, and J. A. Benediktsson. 2016. "Generalized Differential Morphological Profiles for Remote Sensing Image

Classification." *IEEE Journal of Selected Topics in Applied Earth Observations & Remote Sensing* 9 (4): 1736–1751. doi:10.1109/JSTARS.2016.2524586.

Kuleli, T., A. Guneroglu, F. Karsli, and M. Dihkan. 2011. "Automatic Detection of Shoreline Change on Coastal Ramsar Wetlands of Turkey." *Ocean Engineering* 38 (10): 1141–1149. doi:10.1016/j.oceaneng.2011.05.006.

La Monica G. B., E. Petrocchi, M. C. Salvatore, R. Salvatori, and R. Casacchia. 2008. "A New Approach to Detect Shoreline from Satellite Images." Beach Erosion Monitoring, Results from BEACHMED-e/OpTIMAL Project. Firenze: Nuova Grafica Fiorentina Italy.

Liu, H., and K. C. Jezek. 2004a. "A Complete High-resolution Coastline of Antarctica Extracted from Orthorectified Radarsat SAR Imagery." *Photogrammetric Engineering & Remote Sensing* 70 (5): 605–616.

Liu, H., and K. C. Jezek. 2004b. "Automatic Extraction of Coastline from Satellite Imagery by Integrating Canny Edge Detection and Locally Adaptive Thresholding Methods." *International Journal of Remote Sensing* 25 (5): 937–958.

Maiti, S., and A. K. Bhattacharya. 2009. "Shoreline Change Analysis and Its Application to Prediction: A Remote Sensing and Statistics Based Approach." *Marine Geology* 257 (1): 11–23. doi:10.1016/j.margeo.2008.10.006.

Matheron, G. 1975. *Random Sets and Integral Geometry*. New York: John Wiley.

Nguyen, H. H., C. McAlpine, D. Pullar, K. Johansen, and N. C. Duke. 2013. "The Relationship of Spatial–Temporal Changes in Fringe Mangrove Extent and Adjacent Land-use: Case Study of Kien Giang Coast, Vietnam." *Ocean & Coastal Management* 76: 12–22. doi:10.1016/j.ocecoaman.2013.01.003.

Parker, J. R. 1996. *Algorithms for Image Processing and Computer Vision*. New York: Wiley.

Puissant, A., S. Lefèvre, and J. Weber. 2008. "Coastline Extraction in VHR Imagery Using Mathematical Morphology with Spatial and Spectral Knowledge." The SPRS Congress, Beijing, China, July 3–11.

Qu, J. and C. Wang. 2002. "A Multi-threshold Based Morphological Approach for Extraction Coastal Line Feature in Remote Sensed Images." Pecora 15/Land Satellite Information IV/ISPRS Commission I/FIEOS Conference, Denver, Colorado, November 10–14.

Serra, J. P. 1982. *Image Analysis and Mathematical Morphology*. London: Academic Press.

Seul, M., L. O'Gorman, and M. J. Sammon. 2000. *Practical Algorithms for Image Analysis: Description, Examples and Code*. New York: Cambridge University Press.

Soille, P. 2004. *Morphological Image Analysis: Principles and Applications*. Berlin Heidelberg: Springer-Verlag.

Wang, C., J. Zhang, and Y. Ma. 2010. "Coastline Interpretation from Multispectral Remote Sensing Images Using an Association Rule Algorithm." *International Journal of Remote Sensing* 31 (24): 6409–6423. doi:10.1080/01431160903413739.

White, K., E. Asmar, and M. Hesham. 1999. "Monitoring Changing Position of Coastlines Using Thematic Mapper Imagery, and Example from the Nile Delta." *Geomorphology* 29 (1): 93–105. doi:10.1016/S0169-555X(99)00008-2.

Zhou, Y., L. Jiancheng, S. Zhanfeng, H. Xiaodong, and H. Yang. 2014. "Multiscale Water Body Extraction in Urban Environments from Satellite Images." *IEEE Journal of Selected Topics in Applied Earth Observations & Remote Sensing* 7 (10): 4301–4312. doi:10.1109/JSTARS.2014.2360436.